DOI: 10.1111/jace.12194

Micromolding of Calcium Carbonate Using a Bio-Inspired, Coacervation-Mediated Process

Paulina Kaempfe, Victor R. Lauth, Torben Halfer, Laura Treccani, Michael Maas,† and Kurosch Rezwan

Advanced Ceramics, University of Bremen, Am Biologischen Garten 2, 28359 Bremen, Germany

Based on a novel approach that takes into account the coacervation of calcium and poly(acrylic acid) (PAA), we were able to biomimetically produce molded micropatterned parts from amorphous calcium carbonate (ACC) particles. We studied the time- and concentration-dependent growth of Ca^{2+}/PAA coacervate droplets using dynamic light scattering (DLS) and turbidity measurements. Applying these results for the generation of high amounts of unstable ACC particles, we were able to produce slurries that could be molded into micropatterned casts. The obtained slurries contained both micrometer sized ACC particles and smaller nano-sized particles. When both types of particles were used for molding, materials with a high surface roughness could be produced, while the micropatterns of the molds could not be reproduced properly. However, by removing the bigger particles from the slurry using only the smaller, unstable, ACC particles, good reproduction of the micropatterns could be achieved, yielding smooth surfaces with a high surface area. The processing route represents a versatile platform for the bottom-up preparation of micropatterned ceramics on the basis of calcium carbonate.

I. Introduction

Biomineralization has long since fascinated scientists and engineers alike, owing to the extraordinary mechanical properties and intricate design of mineralized tissues. Contrary to the jagged edges of crystals grown under equilibrium conditions, biominerals often exhibit non-equilibrium morphologies like curved shapes while at the same time being single-crystalline. One example is the spicule of sea urchin larvaes.[1,2] Depending on the age of the spicule, it consists of calcite or amorphous calcium carbonate (ACC). Other examples for calcium carbonate ($CaCO_3$) based biominerals with extensive non-equilibrium morphologies are found in coccoliths, foraminiferans or brittle stars.[3] Besides calcium phosphate, calcium carbonate is the biomineral that is most frequently studied in the scientific literature. The discovery of amorphous precursors to the more stable crystal phases of $CaCO_3$ like calcite, aragonite or vaterite has sparked a debate about the nature and general importance of these precursors.[4–7] In recent years, the attention has been focused on the interaction of process-directing agents such as polyanions with biominerals during the nucleation stages that stabilize these amorphous precursors. One example from nature is the formation mechanism of coccoliths.[8,9] Here, Marsh could show that the first steps of coccolithophore formation proceed through the accumulation of calcium rich anionic polysaccharide nanoparticles in vesicles that fuse with vesicles containing an organic matrix, the so-called base plate rim. In turn, the precursor particles accumulate and merge on the surface of the organic matrix and crystallize into calcite. This example also shows the importance of polyanionic additives that can play a role as process directing agents in biomineralization. A possible liquid precursor has been identified by Gower and Odom.[10] The polymer induced liquid precursor (PILP) phase is described as a liquid-liquid phase separation occurring after the gas phase addition of carbonate into a calcium solution containing small amounts of polyanions like poly(aspartate) or poly(acrylic) acid.[11] Polymer-mineral complexes phase separate in the form of unstable liquid droplets that readily coalesce and over time transform into ACC.[12,13]

The applicability of the PILP process in molding calcium carbonate has been e.g., demonstrated replicating sea urchin spines[1] and other shapes[14,15] on the micron scale and has been expanded to the introduction of calcium phosphate into a collagen matrix.[16] The different roles of hydrophilic polymers during the mineralization of $CaCO_3$ have been extensively investigated by Gebauer *et al.*[17] and Cölfen[18] The only related work that mentions complex coacervation of poly (acrylic acid) (PAA) with calcium ions is a paper by McKenna *et al.*[19] Here, though complex coacervation is discussed jointly with other mineralization strategies, the necessary conclusions, especially the time dependence of the system, have not been consequently applied. Time dependence of coacervation-mediated mineralization (though again not by name) was demonstrated by Huang *et al.* describing the formation of $CaCO_3$ particles from a coacervate phase.[20]

Coacervation is a term that was first introduced by Kruyt and Bungenberg de Jong in 1929.[21,22] As a colloidal phenomenon it describes the demixing or liquid-liquid phase separation of lyophilic colloids into a two-phase system. It is called complex coacervation when at least one constituent is a charged colloid that associates (forms a complex) with an oppositely charged ion, molecule or colloid. A classical example for a complex coacervation system is gum arabic and gelatin,[23] but complex coacervation has also been demonstrated with polyanionic polymers like poly(acrylic) acid and multivalent ions, e.g., Ca^{2+}.[24] Coacervation results in the formation of one phase having a high colloid concentration and one having a very low concentration. Coacervate formation proceeds through homogeneous demixing leading to the formation of a transient droplet phase.[25] This droplet phase (the droplets being rich in colloids) is what sets coacervates apart from other demixing processes like flocculation that result in the formation of solid aggregates. Coacervate droplets are unstable and over time undergo Ostwald ripening until they form one cohesive, separate phase in the resulting two-phase system.[26] The theory of complexation has been explored by Burgess on the basis of the work of Overbeek and Voorn,[27] discussing, next to the electrostatic interaction of the colloids, the role of entropy contributions to the demixing process. Coacervates have found widespread use in the encapsulation of flavors and other active ingredients.[23,28–30]

L. Gauckler—contributing editor

Manuscript No. 32063. Received September 25, 2012; approved December 30, 2012.
†Author to whom correspondence should be addressed. e-mail: michael.maas@uni-bremen.de

In this work we propose that by looking at these precursor phases as complex coacervates of PAA with calcium ions we gain a new level of control over polyanion-mediated mineralization with PAA. As described above, coacervation of Ca^{2+} ions and PAA molecules leads to the formation of droplets that sequester from the continuous aqueous polymer solution. This phase separation can be quenched by adding carbonate ions leading to the transformation of coacervate droplets into particles consisting of PAA and ACC.[20] The formation of the coacervate phase renders the volume phase low on PAA, but, depending on the initial ion concentrations, leaves behind a high supersaturation of calcium and carbonate. This leads to the PAA-mediated nucleation of small, unstable ACC particles in the volume phase, jointly with the emergence of coacervates. If the reactant concentrations and the coacervation time are carefully controlled, fairly high concentrations of coacervate droplets and small $CaCO_3$ particles can be produced. We demonstrate the applicability of these concepts by producing micropatterned, macroscopic casts of calcium carbonate using polydimethylsilane (PDMS) molds. Removing the micrometer sized coacervate droplets from the solution (e.g., by centrifugation) gives rise to dispersions containing only the nano-sized, unstable ACC particles. The nano-sized particles can in turn be centrifuged and poured into a micropatterned PDMS mold for the production of micropatterned ACC parts with an extremely low surface roughness. By giving the bigger particles (derived from the coacervate droplets) into a pre-defined mold, the droplets partially merge, with the smaller particles acting as a glue, forming a cohesive green body (unsintered macroscopic compound).

II. Experimental Section

Materials

The following chemicals were purchased from the indicated suppliers and used without further purification: $CaCl_2$ (Sigma Aldrich, Taufkirchen, Germany, purity $\geq$96%), Na_2CO_3 (Sigma Aldrich, purity $\geq$99.5%), polyacrylate sodium salt (PAANa, M_W = 8000 g/mol, 45 w% in water; Sigma Aldrich). All experiments were carried out using double deionized water with a conductivity of 0.04 µS/cm obtained from a Synergy® apparatus (Millipore, Darmstadt, Germany). The molding forms (PDMS, Sylgard® 184 silicone elastomer, Dow Corning, Wiesbaden, Germany) were prepared as described in the literature.[31]

Synthesis of amorphous calcium carbonate (ACC) green bodies

For a continuous preparation of the ACC–PAA dispersion we used a peristaltic pump (Ismatec, Germany) with Tyrgon® tubes (2.54 mm) as a tube reactor. The flow rate was adjusted to 30 mL/min. Aqueous solutions of PAA were prepared with concentrations from 100 to 1,000 mg/mL. Using the pump system, PAA and $CaCl_2$ solutions were mixed. After various time periods (immediately up to an hour) an aqueous solution of Na_2CO_3 was added to the PAA/$CaCl_2$ solution, always keeping the same final concentration of $[Ca^{2+}] = [CO_3^{2-}]$ ions ranging from 2 to 50 mM. After a mixing time of 10 sec, the cloudy dispersions were immediately centrifuged (20 min at 250 g) in order to separate smaller particles and coacervate droplets. The supernatant was centrifuged for a second time (20 min at 610 g) to separate the smaller particles from water. After the removal of the supernatant the viscous, white residue was pipetted into a O_2 plasma treated PDMS mold dried at ambient conditions (21°C, 30% r.h.) for 24 h. The shrinkage of the samples due to water loss was about 30%. O_2 plasma treatment was carried out using low-pressure plasma with 50 W power generator for 2 min and an operating pressure of 0.3 mbar.

Characterization

X-ray diffraction analysis (XRD) was carried out using a JSO-Debyeflex 2002 device, with Cu$K\alpha$ radiation (λ = 1.542 Å). The samples were ground to form a small particle size powder and scanned for 2 s per degree from 5° to 70°. For dynamic light scattering (DLS), a Microtrac UPA 150 apparatus was used. The correlation function was processed using the density and refraction index parameters corresponding to PAA, $CaCO_3$, and H_2O. The autocorrelation function was fitted using the Mie method. Absorbance analysis was measured in a Dr. Lange X ion 500 machine at 450 nm.

Additionally, the dry products were analyzed by TGA (oxidative conditions, air flow = 2 L/h). Both small and large particles (measured individually) consist of 6%–7% of PAA, while the smaller particles contained less water (6 wt%) as the bigger ones (13 wt%), probably due to the inclusion of water in the bigger particles.

The specific surface area (S_{BET}) of the samples was determined by nitrogen adsorption (Belsorp-Mini, Bel Japan, Osaka, Japan), using the BET-method.[32] For titration experiments the titration manager TitraLab® TIM840 was used. The morphology of the droplets and the molded green bodies were evaluated by scanning electron microscopy (SEM; Zeiss, SUPRA 40), with an acceleration voltage of 15 kV and sputtering with gold for 30 s.

III. Results

The complex coacervation process between Ca^{2+}-ions and PAA is fundamental to the mechanisms for micro-molding ACC. For this reason, first, the complexation and demixing of Ca^{2+} and PAA was studied. Figure 1 depicts the time-dependent mechanism for calcium carbonate formation based on the demixing of the coacervate phase. Demixing proceeds directly after the addition of calcium chloride to the aqueous PAA solution via the formation of small droplets of the Ca^{2+}/PAA complex rich phase [Fig. 1(a)]. After nucleation [Fig. 1(aI)], the droplets rapidly grow into micron-sized droplets that are easy to identify via DLS and turbidity measurements [Fig. 1(aII)]. If left unperturbed, the droplets undergo Ostwald ripening and after a period of 3 h the whole system is separated into two continuous phases [Fig. 1(aIII)]. As a result, the lower phase is highly viscous and contains a high concentration of Ca^{2+}/PAA coacervates, while the upper phase is a polymer-poor aqueous solution. Depending on the time of addition, adding sodium carbonate solution during the different stages of demixing leads to the formation of different types of calcium carbonate [Fig. 1(b)].

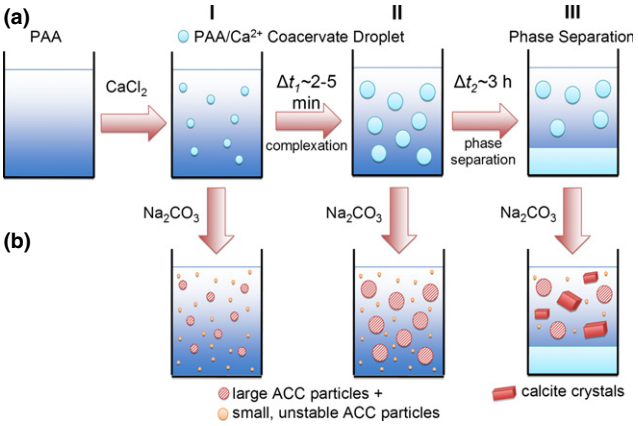

Fig. 1. Scheme of the complex coacervation system: (a) the PAA/Ca^{2+}-system shows time-dependent growth of the coacervate droplets; (b) Addition of the Na_2CO_3 solution after different growth times (I, II, III) to the PAA/Ca^{2+}-system shows different kinds of solids ($CaCO_3$).

If the Na_2CO_3 solution is added directly after the addition of $CaCl_2$, while the coacervation droplets are still very small, the resulting ACC particles are small, too [Fig. 1(bI)]. Next to these ACC particles, much smaller particles ($d \approx 8$ nm) form, due to the high supersaturation of ions and the presence of free PAA-molecules. If the period of time between the formation of the coacervate droplets and the addition of Na_2CO_3 is longer, the bigger ACC particles that are derived from the growing coacervate droplets increase in size [Fig. 1(bII)]. After the separation into two bulk phases, next to the ACC particles, calcite crystals form in the upper part of the solution, due to the low concentration of PAA in the polymer-poor phase [Fig. 1(bIII)].

The time-dependent growth of the Ca^{2+}/PAA coacervate droplets prior to the addition of Na_2CO_3 also strongly depends on the concentration of both reactants. Figure 2 illustrates the growth of these droplets as a function of concentration and time. Figure 2(a) shows the increasing size of coacervate droplets at different PAA concentrations (100–1000 mg/L) with a fixed $CaCl_2$ concentration of 20 mM (measured with DLS). Within the first 10 min in all observed systems the droplet size of the Ca^{2+}/PAA complex increases rapidly. If the initial concentration of PAA is increased, the droplet size at the beginning of the process also increases. During the observed period of time the droplets grow with a similar rate at all concentrations. If the concentration of PAA is kept at 1000 mg/L and the amount of $CaCl_2$ is varied (10–50 mM), the droplet growth is a function of the initial concentration of the reactants [Fig. 2(b)]. In comparison to Fig. 2(a), turbidity measurements at 450 nm also show that within the first 10 min the droplets grow rapidly, followed by a slow decline in turbidity. Additionally, during the initial growth phase, the turbidity increases as a function of the starting concentrations of the reactants [Fig. 2(c)]. After the initial growth phase, the turbidity decreases constantly. This effect is based on the metastable nature of the coacervation system. The coacervate droplet dispersion breaks when the coacervate droplets exceed a specific size, leading to sedimentation and ultimately the formation of two discrete phases. It was not possible to monitor this effect using DLS because of the onset of polydispersity of the dispersions after 10 min as a result of Ostwald ripening of the droplets. A turbidity phase diagram, 2 min after preparation of the coacervation system is presented in Fig. 2(d). The region of highest turbidity shows the biggest coacervate droplets in the dispersion. Accordingly, coacervate droplet formation and growth are favored with increasing concentrations of PAA and $CaCl_2$.

In order to gain insight into Ca^{2+}/PAA complex formation, the pH variation upon titration of $CaCl_2$ with PAA was investigated. With similar experiments, Wang and Cölfen demonstrated that the addition of a $BaCl_2$ solution to a PAA solution showed a pH decrease due to proton release upon Ba^{2+} coordination to the $RCOO^-$ groups in PAA.[33] This reveals a strong complexation between these two components. In this respect, the behavior of Ca^{2+} is comparable to that of barium salt. Figure 3 displays the pH variation of PAA solution upon titration with $CaCl_2$, showing the formation of the PAA/Ca^{2+} complex. Since sodium-acrylate has a pK_B value of 9.45, the PAA- solution is slightly basic (pH 9.3). During the titration with Ca^{2+}, the pH value decreases because of the formation of $(RCOO)_2Ca$, leading to the dissociation of protons from the carboxylate groups. At the beginning of the titration, the pH decrease is very pronounced which indicates fast complexation of the added Ca^{2+}-ions. After the addition of more than 1.6 mL $CaCl_2$-solution the slope decreases due to the saturation of the carboxylate groups with Ca^{2+}.

Based on the observations on the coacervation of Ca^{2+}/PAA, it can be shown that the particle size of the ACC particles depends on the time of the addition of sodium carbonate to the coacervate droplet dispersion [Fig. 1(b)].[20] Figure 4(a)

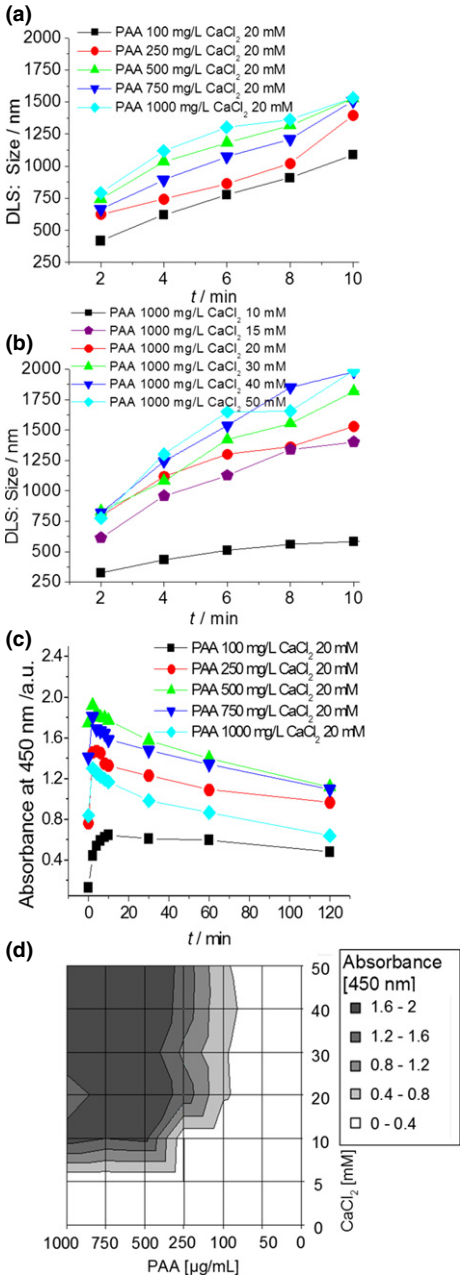

Fig. 2. Examples of the time-dependent coacervate droplet growth [see also Fig. 1(a)]: (a) dynamic light scattering (DLS) results of droplet diameters as a function of the initial PAA concentration ([PAA] = 100–1000 µg/mL, [$CaCl_2$] = 20 mM), (b) and as a function of the $CaCl_2$ concentration ([$CaCl_2$] = 10–50 mM, [PAA] = 1000 µg/mL), (c) turbidity measurement as a function of the PAA concentration ([PAA] = 100–1000 µg/mL, [$CaCl_2$] = 20 mM), (d) Turbidity Phase diagram at 450 nm 2 min after preparation of the system ([PAA] = 50–1000 µg/mL, with [$CaCl_2$] = 20–50 mM).

illustrates the transformation of coacervate droplets into ACC particles with turbidity measurements of the system PAA/Na_2CO_3/$CaCl_2$ at the time of the addition of sodium carbonate. Na_2CO_3 was added 2 min after the addition of $CaCl_2$. Based on the initial concentration of the reactants, the dispersions show a moderate increase in turbidity within the first 30 min. This increase is most likely due to the change in optical density of the coacervate droplets as they transform into ACC particles. According to Huang *et al.*, growth of the coacervate droplets is quenched by the addition of carbonate ions.[20] In the following time frame the turbidity changes only insignificantly. The slight decrease in turbidity is a result of the sedimentation of the particles. Figure 4(b) shows a turbidity phase diagram at 450 nm

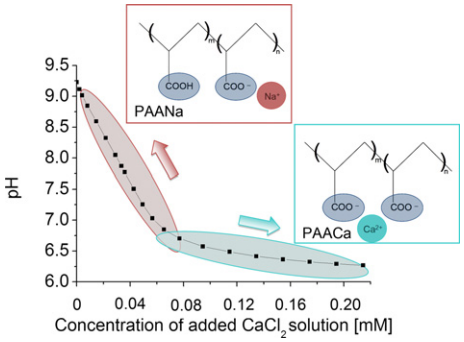

Fig. 3. pH variation of PAA (20 mL, [PAA] = 750 μg/mL, pH 9.25) solution upon titration with $CaCl_2$ ([$CaCl_2$] = 40 mM, pH 6.52) shows the formation of the PAA/Ca^{2+} complex. Insets: sodium association to PAA at the beginning of the titration, calcium complexation as a result of the titration.

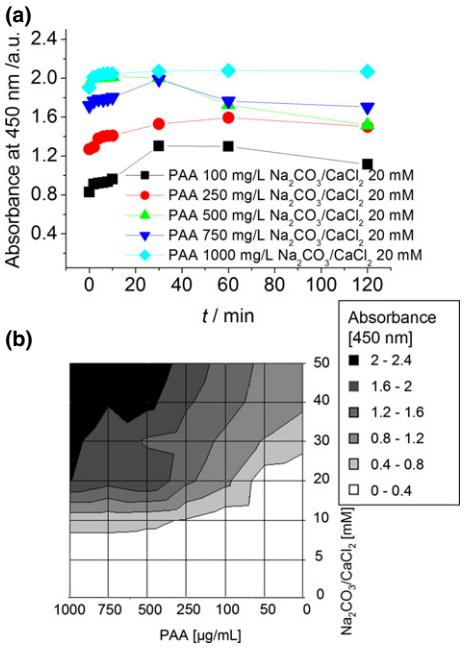

Fig. 4. Examples of the time-dependent growth of the coacervate droplets [see also Fig. 1(b)]: (a) turbidity measurement as a function of the $Na_2CO_3/CaCl_2$ concentration ([PAA] = 100–1000 μg/mL, [$Na_2CO_3/CaCl_2$] = 20 mM); (b) Turbidity phase diagram at 450 nm of the system PAA with $Na_2CO_3/CaCl_2$ ([PAA] = 50–1000 μg/mL [$Na_2CO_3/CaCl_2$] = 0.2–50 mM), 2 min after the addition of Na_2CO_3.

2 min after the addition of Na_2CO_3. Analogous to Fig. 2(d) the size of the ACC particles increases with the concentration of all reactants.

Figure 5(a) shows the dried dispersion 5 min after preparation, directly before the first centrifugation step. The larger ACC particles ($d \approx 1.5$–2.0 μm) are clearly visible next to the smaller particles. DLS measurements of the mixed dispersions showed three main peaks at about 20, 150, and 800 nm with comparable volume fractions [Fig. 6(a)]. For the dispersions containing only small nanoparticles both the number- and volume-weighted results showed that most of the nanoparticles are in the order of 8 nm [Fig. 6(b)]. Although the multimodal fit provides only semi-quantitative results, it still substantiates our description of the dispersions.

Additionally, the size of the smaller particles can be validated from SEM and TEM [Fig. 5(b) and (c)] micrographs. The smaller particles adsorb to the larger ACC particles, acting as a glue between the larger particles. After centrifugation, only the smaller particles remain dispersed [Fig. 5(b)].

Since coacervate formation occurs in a wide range of reactant concentrations, coacervation mediated production of ACC can yield high amounts of particles. Furthermore, the size of the ACC particles can be controlled via the coacervation time. As discussed above, next to coacervation-mediated formation of ACC-particles, smaller, unstable particles form due to the high supersaturation of the mineralizing solutions. These aspects can be utilized for molding micropatterned ceramics.

For the molding experiments, macroscopic (5 mm × 5 mm) PDMS molds were used that incorporated micropatterns on one surface. The molding process is schematically described in Fig. 7 (Fig. 7 proceeds from Fig. 1(bII) onward). After the addition of sodium carbonate (Fig. 7, I), the first centrifugation step is carried out after 5 min. After the first centrifugation step (Fig. 7, II) it is possible to isolate the smaller particles in the supernatant and discard the residue with the bigger ACC particles. A second centrifugation step at 610 g for 20 min allows the separation of the smaller particles from the aqueous solution (Fig. 7, III).

For molding the ACC nanoparticles, the viscous, milky residue is transferred into a PDMS-mold with a pipette. In case of a high amount of large ACC particles (after the first centrifugation step, Fig. 7, II) the molding process does not lead to a well-defined and flat surface. In contrast, the residue of the second centrifugation step (containing small, unstable ACC particles) forms a nearly crack-free and planar surface with well-defined contours. Exemplary results of the molding experiments of ACC are shown in Fig. 8. In general, we were able to produce parts that exhibited dimensions of several millimeters and that had a micropattern embedded on one of the surfaces (an example is shown in Fig. 7). In the presence of large ACC particles, taking the residue after the first centrifugation step, the molded ACC green body shows irregular edges without a well-structured reproduction of the PDMS form [Fig. 8(a)]. The surface is rough and the ACC particles are agglomerated. Since the sample portrayed in Fig. 8(A) has been dried for several days, the

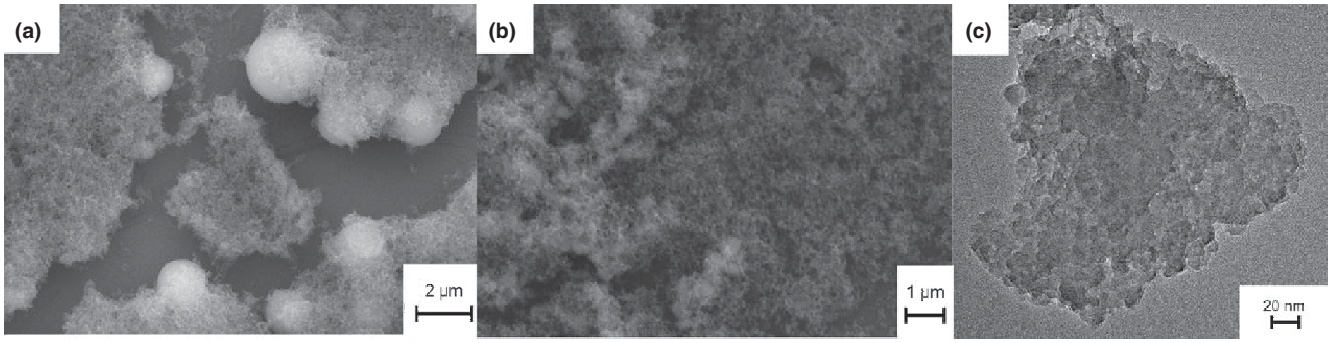

Fig. 5. SEM (a, b) and TEM (c) micrographs of the dried liquid phases of dispersed $CaCO_3$ ([$Na_2CO_3/CaCl_2$] = 40 mol/L) with PAA ([PAA] = 750 μg/mL); comparison between coacervate droplets and smaller particles; (a) 5 min. after preparation (Fig. 7, I), (b, c) supernatant after the first centrifugation step (Fig. 7, II).

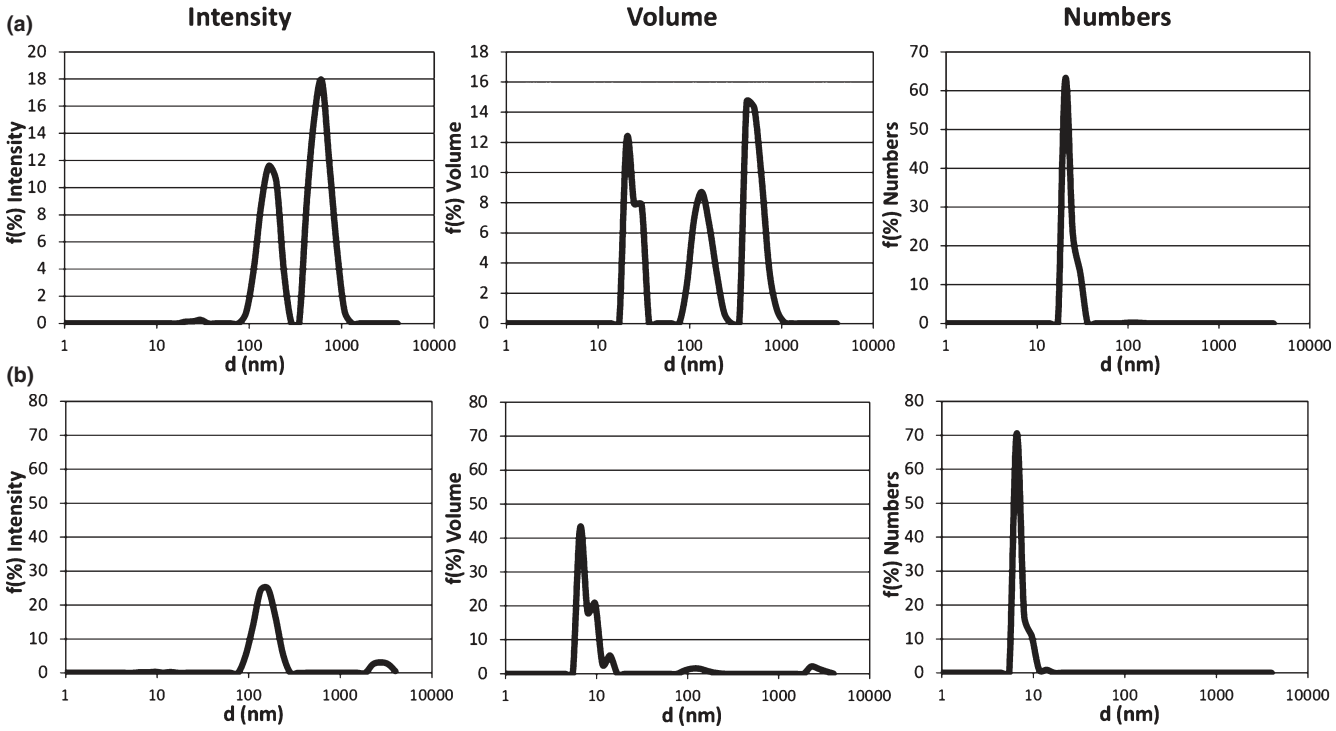

Fig. 6. Dynamic light scattering (DLS) measurements dispersion of both small and large particles (a) before and (b) after the first centrifugation step. The NNLS fit of the cumulant function is weighted by intensity, volume, and numbers.

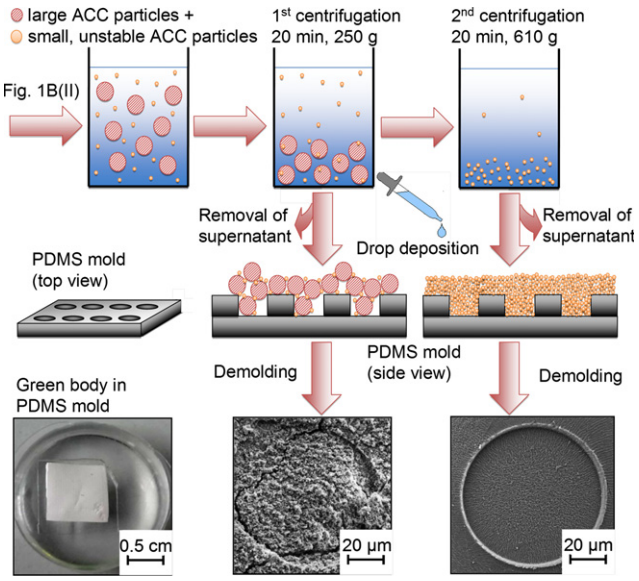

Fig. 7. Coacervation-mediated molding of amorphous calcium carbonate (ACC) (sequel to Fig.1(b),II): (I) dispersion after preparation (Fig.1(b), II), (II) after the first centrifugation step, (III) after the second centrifugation step. After the removal of the supernatant the residues are transferred via pipette to the PDMS mold.

spherical larger particles [compare Fig. 5(a)] are covered with a thick layer of smaller particles that have merged upon drying. This leads to the formation of an uneven layer that coats and firmly links the larger particles. However, the dispersion containing the larger ACC particles is ill-suited for the reproduction of micropatterns.

When the larger particles are removed from the dispersion by centrifugation, molding the smaller particles (using the residue after the second centrifugation step) generates well defined micropatterned ACC green bodies with an extremely low surface roughness [Fig. 8(B)]. The smaller particles partially merge to form a smooth surface. The morphology of the smaller particles in the mold is more angular compared to the morphology of the particles from the dispersion [Fig. 5(B)] which might again be caused by the drying and demolding process. XRD-analysis revealed that all samples contain ACC only with some traces of calcite in some samples. The specific surface area of the different sample types was also determined. A sample consisting of a mixture of both particle sizes seen on Fig. 8(a) has a S_{BET} of about 50 m^2/g. The specific surface area is almost doubled in the presence of only small particles in the mold (about 80 m^2/g). BET nitrogen-adsorption isotherms showed no distinct micro- or meso-porosity of the samples.

The resulting green bodies were fragile and need to be transformed into a more stable material before being applicable as ceramic materials. A first approach is the transformation of ACC into the thermodynamically more stable calcite. Here, the challenge lies in maintaining the micropattern of the molds during the transformation and at the same time to firmly link the emerging crystals. This is a complex topic that is part of ongoing research.

IV. Discussion

The coacervation-mediated mineralization process can be divided into two parts. The first part is the mineralization of the coacervate droplets themselves. The droplets contain very high concentrations of PAA and Ca^{2+}. When CO_3^{2-} is introduced into the PAA/Ca^{2+} system, the coacervate droplets quickly mineralize into ACC particles. In this case, the ACC phase is favored by the presence of PAA and by the fast reaction at high supersaturation.

The second part of coacervation-mediated mineralization is the formation of unstable particles in the bulk phase. The PAA concentration in the polymer-poor bulk phase is insufficient to form coacervates but still interacts with $CaCO_3$ nuclei and clusters, that form due to the high concentration of ions.

Generally, the impact of additives on calcium carbonate crystallization is very complex. Additives can e.g., act in the prenucle-

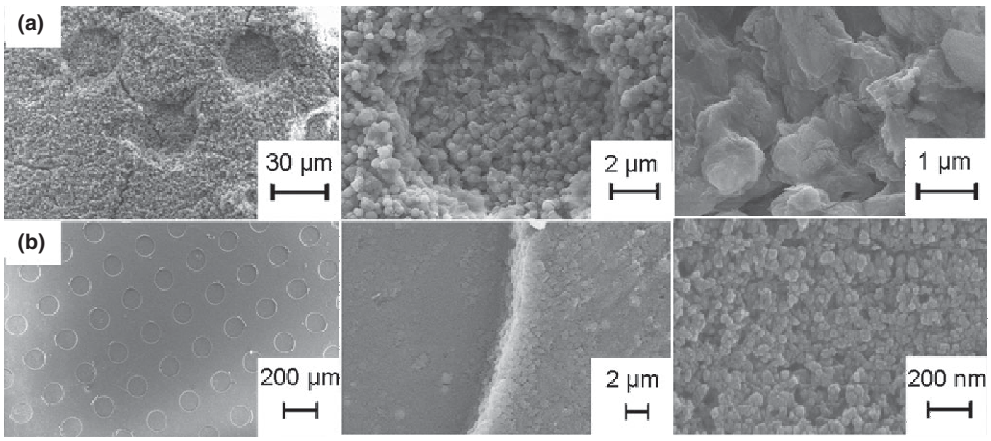

Fig. 8. SEM micrographs of molded amorphous $CaCO_3$ ([Na_2CO_3/$CaCl_2$] =40 mM) with PAA ([PAA] = 750 µg/mL) at different magnifications: (a) after the first centrifugation step (Fig. 7, II), (b) after the second centrifugation step (Fig. 7, III).

ation stage, by adsorption on crystal growth planes or by partially suppressing nucleation.[17] These different kinds of interactions are described in great detail in the literature.[18] Using the balance between coacervation-mineralization and polyanion-mediated nucleation, we were able to demonstrate the production of bulk amounts of differently sized ACC nanoparticles.

Interestingly, small droplets of calcium/polyanions complexes are also found in nature, e.g., during the above mentioned formation of coccolithophores.[9,34] Here, it seems that coacervate droplets of the acidic polysaccharide PS2 and calcium ions are extruded into vesicles and then mineralized via the addition of carbonates. It is important to note that these droplets are able to exist at extremely high concentration in vesicles, which is compatible with our description of the coacervation system.

V. Conclusions

In summary, ACC was successfully prepared in bulk via a coacervation-mediated process using calcium chloride, sodium carbonate and PAA. Using DLS and turbidity measurements, we studied the time- and concentration-dependent growth of Ca^{2+}/PAA coacervate droplets. Applying these results for the generation of high amounts of unstable ACC particles, we were able to produce slurries that could be molded into micropatterned PDMS molds. The slurries contained both micrometer sized ACC particles and smaller nano-sized ACC particles. If both types of particles were used for molding, materials with a high surface roughness could be produced, although the micropatterns of the molds could not be reproduced properly. If the bigger particles were removed from the slurry using only the smaller, unstable $CaCO_3$ particles, good reproduction of the micropatterns could be achieved yielding smooth surfaces with a high surface area. The coacervation system is a versatile platform for the bottom-up preparation of ceramics on the basis of calcium carbonate. Further studies will focus on the long-time behavior of the ACC casts and the preparation of capsule materials based on this approach.

References

[1]X. Cheng and L. B. Gower, "Molding Mineral Within Microporous Hydrogels by a Polymer-Induced Liquid-Precursor (PILP) Process," *Biotechnol. Prog.*, **22**, 141–9 (2006).

[2]E. Beniash, J. Aizenberg, L. Addadi, and S. Weiner, "Amorphous Calcium Carbonate Transforms Into Calcite During sea Urchin Larval Spicule Growth," *Proc. R. Soc. Lond. B*, **264**, 461–5 (1997).

[3]L. B. Gower, "Biomimetic Model Systems for Investigating the Amorphous Precursor Pathway and Its Role in Biomineralization," *Chem. Rev.*, **108**, 4551–627 (2008).

[4]B. R. Heywood and S. Mann, "Template-Directed Nucleation and Growth of Inorganic Materials," *Adv. Mater.*, **6**, 9–20 (1994).

[5]E. DiMasi, M. J. Olszta, V. M. Patel, and L. B. Gower, "When is Template Directed Mineralization Really Template Directed?" *Cryst. Eng. Commun.*, **5**, 346–50 (2003).

[6]M. Fricke and D. Volkmer, "Crystallization of Calcium Carbonate Beneath Insoluble Monolayers: Suitable Models of Mineral–Matrix Interactions in Biomineralization?" *Biomineralization I, Top. Curr. Chem.*, **270**, 1–41 (2007).

[7]M. Faatz, F. Gröhn, and G. Wegner, "Amorphous Calcium Carbonate: Synthesis and Potential Intermediate in Biomineralization.," *Adv. Mater.*, **16**, 996–1000 (2004).

[8]R. J. Park and F. C. Meldrum, "Shape-Constraint as a Route to Calcite Single Crystals With Complex Morphologies.," *J. Mater. Chem.*, **14**, 2291–6 (2004).

[9]M. E. Marsh, "Polyanion-Mediated Mineralization—Assembly and Reorganization of Acidic Polysaccharides in the Golgi System of a Coccolithophorid Alga During Mineral Deposition," *Protoplasma*, **177**, 108–22 (1994).

[10]L. B. Gower and D. J. Odom, "Deposition of Calcium Carbonate Films by a Polymer-Induced Liquid-Precursor (PILP) Process," *J. Cryst. Growth*, **210**, 719–34 (2000).

[11]M. J. Olszta, D. J. Odom, E. P. Douglas, and L. B. Gower, "A New Paradigm for Biomineral Formation: Mineralization via an Amorphous Liquid-Phase Precursor," *Connect. Tissue Res.*, **44**, 326–34 (2003).

[12]L. Dai, E. P. Douglas, and L. B. Gower, "Compositional Analysis of a Polymer-Induced Liquid-Precursor (PILP) Amorphous CaCO3 Phase," *J. Non-Cryst. Solids*, **354**, 1845–54 (2008).

[13]B. Cantaert, Y.-Y. Kim, H. Ludwig, F. Nudelman, N. Sommerdijk, and F. C. Meldrum, "Think Positive: Phase Separation Enables a Positively Charged Additive to Induce Dramatic Changes in Calcium Carbonate Morphology," *Adv. Funct. Mater.*, **22**, 907–15 (2012).

[14]Y.-Y. Kim, E. P. Douglas, and L. B. Gower, "Patterning Inorganic ($CaCO_3$) Thin Films via a Polymer-Induced Liquid-Precursor Process," *Langmuir*, **23**, 4862–70 (2007).

[15]D. Volkmer, M. Harms, L. Gower, and A. Ziegler, "Morphosynthesis of Nacre-Type Laminated $CaCO_3$ Thin Films and Coatings," *Angew. Chem. Int. Ed.*, **44**, 639–44 (2005).

[16]M. J. Olszta, X. Cheng, S. S. Jee, R. Kumar, Y.-Y. Kim, M. J. Kaufman, E. P Douglas, and L. B. Gower, "Bone Structure and Formation: A new Perspective," *Mater. Sci. Eng., R*, **58**, 77–116 (2007).

[17]D. Gebauer, H. Cölfen, A. Verch, and M. Antonietti, "The Multiple Roles of Additives in CaCO3 Crystallization: A Quantitative Case Study.," *Adv. Mater.*, **21**, 435–9 (2009).

[18]H. Cölfen, "Bio-Inspired Mineralization Using Hydrophilic Polymers," *Biomineralization II, Top. Curr. Chem.*, **271**, 1–77 (2007).

[19]B. J. McKenna, J. H. Waite, and G. D. Stucky, "Biomimetic Control of Calcite Morphology With Homopolyanions," *Cryst. Growth Des.*, **9**, 4335–43 (2009).

[20]S.-C. Huang, K. Naka, and Y. Chujo, "A Carbonate Controlled-Addition Method for Amorphous Calcium Carbonate Spheres Stabilized by Poly (Acrylic Acid)s," *Langmuir*, **23**, 12086–95 (2007).

[21]H. Bungenberg de Jong, "Crystallisation–Coacervation–Flocculation.," *Colloid Sci.*, **2**, 232–58 (1949).

[22]H. Bungenberg de Jong and H. Kruyt, "Coacervation (Partial Miscibility in Colloid Systems)," *Proc. K. Ned. Akad. Wet.*, **32**, 849–56 (1929).

[23]C. G. de Kruif, F. Weinbreck, and R. de Vries, "Complex Coacervation of Proteins and Anionic Polysaccharides," *Curr. Opin. Colloid Interface Sci.*, **9**, 340–9 (2004).

[24]H. Bungenberg de Jong, "Complex Colloid Systems," *Colloid Sci.*, **2**, 335–432 (1949).

[25]R. Arshady, "Microspheres and Microcapsules, a Survey of Manufacturing Techniques Part II: Coacervation.," *Polym. Eng. Sci.*, **30**, 905–14 (1990).

[26]P. L. Madan, "Microencapsulation I. Phase Separation or Coacervation," *Drug. Dev. Ind.*, **4**, 95–116 (1978).

[27]J. T. G. Overbeek and M. J. Voorn, "Phase Separation in Polyelectrolyte Solutions. Theory of Complex Coacervation," *J. Cell. Comp Physiol.*, **49**, 7–26 (1957).

[28]B. J. McKenna, H. Birkedal, M. H. Bartl, T. J. Deming, and G. D. Stucky, "Micrometer-Sized Spherical Assemblies of Polypeptides and Small Molecules by Acid–Base Chemistry," *Angew. Chem. Int. Ed.*, **116**, 5770–3 (2004).
[29]C. Thies, "Microencapsulation of Flavors by Complex Coacervation," chapter 7 in *Encapsulation and Controlled Release Technologies in Food Systems*, edited by J. M. Lakkis. Blackwell Publishing, Ames, IA, (2007). doi: 10.1002/9780470277881.
[30]A. Madene, M. Jacquot, J. Scher, and S. Desobry, Flavour Encapsulation and Controlled Release - a Review, *Int. J. Food Sci. technol.*, **41**, 1–21 (2006).
[31]M. G. Holthaus, M. Kropp, L. Treccani, W. Lang, and K. Rezwan, "Versatile Crack-Free Ceramic Micropatterns Made by a Modified Molding Technique," *J. Am. Ceram. Soc.*, **93**, 2574–8 (2010).
[32]S. Brunauer, P. H. Emmett, and E. Teller, "Adsorption of Gases in Multimolecular Layers," *J. Am. Chem. Soc.*, **60**, 309–19 (1938).
[33]T. Wang and H. Cölfen, "*In Situ* Investigation of Complex $BaSO_4$ Fiber Generation in the Presence of Sodium Polyacrylate. 1. Kinetics and Solution Analysis," *Langmuir*, **22**, 8975–85 (2006).
[34]M. E. Marsh, "Regulation of $CaCO_3$ Formation in Coccolithophores," *Comp. Biochem. Physiol. B*, **136**, 743–54 (2003). □